ELSEVIER

Journal of Molecular Catalysis A: Chemical 150 (1999) 195–203

JOURNAL OF MOLECULAR CATALYSIS A: CHEMICAL

www.elsevier.com/locate/molcata

Synthesis and catalytic performance on methanol conversion of NiAPSO-34 crystals (I): effect of preparation factors on the gel formation

Misook Kang [a,*], Myeong-Heon Um [b], Jong-Yul Park [c]

[a] *Department of Chemical Engineering, Dankook University, San 8, Hannam-dong, Youngsanku, Seoul 140-714, South Korea*
[b] *Department of Industrial Chemistry, Cheonan National Technical College, Cheonan 330-240, South Korea*
[c] *Department of Chemistry, Pusan National University, Pusan 609-735, South Korea*

Received 15 October 1998; accepted 23 March 1999

Abstract

In order to synthesize the NiAPSO-34 crystal with a pure CHA structure having a uniform size and stable catalytic activity, factors having influence on the crystallization at gel preparation were investigated. The results showed that the mixing order of starting materials influences on the crystallization rate. The concentration of the template was related to the morphology of crystals and the crystallinity, while the particle size obtained was controlled by the silica source and the amount of nickel. Moreover, it was elucidated that the mixing orders of starting materials influences on the crystal growth rate. Seed crystal addition (SAPO-34; 0.8 μm) and ultrasonic-wave treatment after the gel formation were effective in decreasing smaller particle size and in narrowing the size distribution.

Keywords: NiAPSO-34; Crystallization rate; Crystallinity; Particle size distribution

1. Introduction

The understanding of the factors controlling the genesis of micropores is of primary importance for a rational design of catalysts. The influence of experimental conditions on gel formation for aluminosilicate molecular sieves has been discussed previously; several works are available discussing the synthesis conditions for the structure types obtained [1–4]. It is very useful to find optimum and reliable conditions of gel formation for the synthesis.

The synthesis and characterization in wide range of metal-substituted silicoaluminophosphate have also been reported in recent years. Although the synthesis of SAPO-type crystals [5,6] has been discussed in the literature, detailed factors affecting the gel preparation have not yet been investigated in detail. These papers report that the metals were incorporated into the framework with tetrahedral coordination at ini-

* Corresponding author. Tel.: +82-2-7092603; Fax: +82-2-7902558; E-mail: msk1205@chollian.dacom.co.kr

1381-1169/99/$ - see front matter
PII: S1381-1169(99)00194-6

tial stage of the gel formation for CoAPSO-5 [6,7]. They discussed the phase of cobalt in gel preparation, but factors having influence on the NiAPSO-34 crystal synthesis were not reported.

As is well known, nickel-containing SAPO-34, having a CHA topology which can be prepared via the synthesis procedure described in Scheme 1, which is used for high ethylene synthesis from methanol, has been subject to great interests. The physicochemical properties of nickel-containing SAPO-34 was sensitive to preparation conditions and much care should be taken in order to obtain high-quality products. When high degrees of heterosubstitution are attempted, it is difficult to attain high-purity samples [8,9]. In addition, minor changes in the synthesis conditions can sensitively lead to the different topology [10]. Under undesirable conditions, the NiAPSO-34 was frequently obtained with impurity assigned to SAPO-5 material.

The crystallization process for NiAPSO-34 crystal was studied in the present work in order to understand the influence on gel chemistry and gel preparation, and an optimum set of experimental conditions for the synthesis of pure NiAPSO-34 structure was suggested.

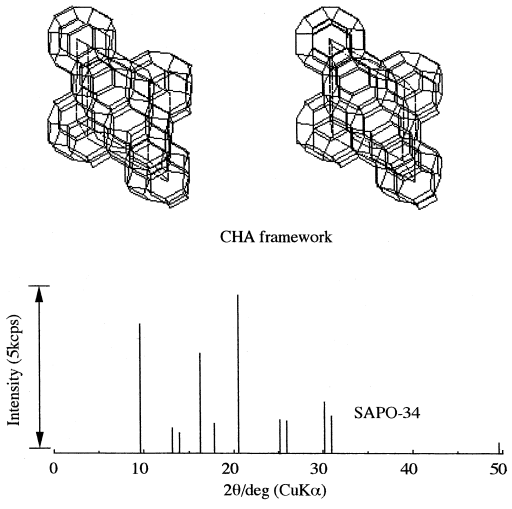

Scheme 1. Structure and XRD pattern of CHA type.

2. Experimental

2.1. Reagents used for gel mixture preparation

Reagents used for the preparation of gel mixture were as follows: 35% aqueous solution of tetraethyl ammonium hydroxide (TEAOH, Aldrich Chemical) was used as the organic template. Aluminum isopropoxide (AIP, Wako), phosphoric acid (85% H_3PO_4, Nacalai Tesque), and nickel nitrate ($Ni(NO_3)_2$ $6H_2O$, Nacalai Tesque) were used as the starting materials of Al, P, and Ni ingredient of NiAPSO-34, respectively. As the silica source, the Cataloid-30 (30% SiO_2, Kasei Tesque), fumed silica (99% SiO_2, Nacalai Tesque), and tetraethyl orthosilicate ($Si(O(C_2H_5)_4$, Wako) were used.

2.2. Sample preparation

The catalyst was prepared by applying the rapid crystallization method introduced by synthesis method of SAPO-34 described in the patent literature [11].

2.3. Factors investigated in gel mixture preparation

2.3.1. Group 1: influence of the mixing order

Mixing order of starting materials of the Al, P, Si, and Ni sources is important essentially to obtain a homogeneous gel mixture. The various mixing methods are summarized in (a), (b) [12], and (c) [13] of Fig. 1. The methods were each named as orderly mixing method (OMM), simultaneous phosphate dropping method (SPDM), and patent method (PM), respectively. The molar composition of gel formed was 0.2 $(TEA)_2O$: 0.2 Al_2O_3: 0.2 P_2O_5: 0.06 SiO_2: 0.0015 NiO: 10 H_2O.

2.3.2. Group 2: influence of the template concentration

The gel mixture was prepared according to the orderly mixing method (OMM) as shown in

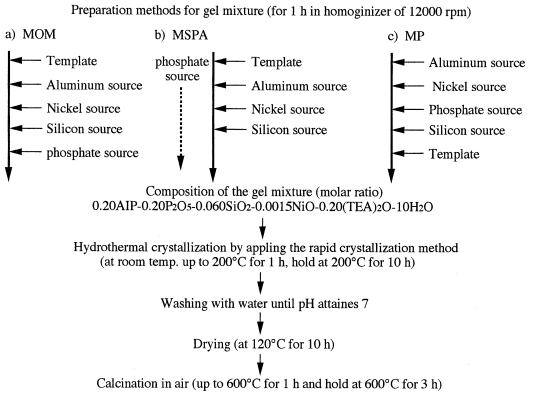

Fig. 1. Preparation methods for the gel mixtures of NiAPSO-34 crystals (for Groups 1–4). (a) Orderly missing method (OMM), (b) simultaneous phosphate dropping method (SPDM), (c) patent method (PM).

Fig. 2. The template concentrations of the gel mixture were 0.10 M, 0.15 M, 0.20 M, 0.25 M, and 0.30 M, fixing the aluminum concentration to 0.20 M. Other ratios were set to 0.2 M Al_2O_3: 0.2 M P_2O_5: 0.06 M SiO_2: 0.0015 M NiO: 10 M H_2O.

2.3.3. Group 3: influence of the nickel amount

The gel mixture was prepared by OMM. The composition of the gel prepared was 0.15 M $(TEA)_2O$: 0.20 M Al_2O_3: 0.20 M P_2O_5: 0.06 M SiO_2: xM NiO: 10 M H_2O. Amount of the added Ni corresponded to the ratio of Si/Ni, as 10, 20, and 40.

2.3.4. Group 4: influence of the silica source and Al / Si ratio

The silica sources were Cataloid-30 (30% SiO_2, Kasei Tesque), fumed silica (99% SiO_2, Nacalai Tesque), and tetraethyl orthosilicate ($Si(OC_2H_5)_4$, Wako). The OMM method again adapted mixing order and Al/Si ratio of the mixture was set to 6.

2.4. Other factors investigated after preparation of gel mixture

2.4.1. Group 5: influence of the addition of seed crystal

Used gel mixture was made by OMM to molar gel composition of 0.2 $(TEA)_2O$: 0.2 Al_2O_3: 0.2 P_2O_5: 0.06 SiO_2: 0.0015 NiO: 10 H_2O. After the gel formation, SAPO-34 seed crystal of 0.5 wt.% was added to the gel mixture, and the final mixture was stirred until homogeneous as shown in Fig. 2.

2.4.2. Group 6: influence of the ultrasonic wave treatment

The sample obtained in Group 5 was further subjected to 100 W ultrasonic treatment at 60°C for 30 min as shown in Fig. 2.

2.4.3. Group 7: influence of the hydrothermal synthesis time

Used gel mixtures were prepared by methods introduced in Group 1. The autoclave containing a gel mixture of known substrate concentrations was placed in temperature-programmed dry oven. Heating rate was 3°C/min until 200°C. The temperature was kept at 200°C, and then the time was checked in each time from 1 h to 5 h during synthesis. The relation between the crystallinity and hydrothermal-treatment time was estimated for three methods described in Section 2.3.1 for the experiments.

2.5. Characterization of samples

Synthesized samples were identified by powder X-ray diffraction analysis (XRD), Shimazu

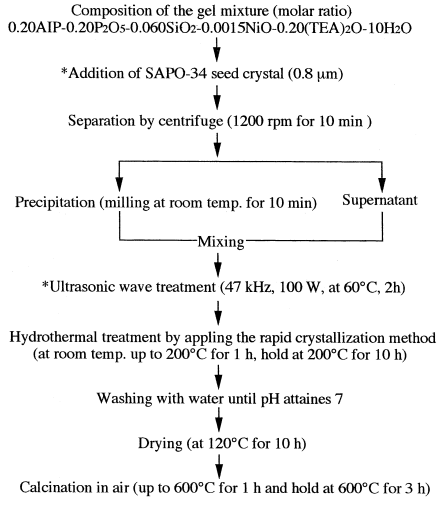

Fig. 2. Treatment process after the gel mixture preparation for synthesis of NiAPSO-34 crystal (for Groups 5 and 6).

XD-DI with nickel filtered Cu Kα radiation (30 kV, 30 mA) at an angle of 2θ range from 5 to 50°. The scan speed was 1°/min and time constant was 1 s. The diffraction angles of 22.0° and 9.7° were selected to discuss the crystallinity of synthesized samples. Particle size and shape were observed by scanning electron microscope (SEM) with Hitachi-Akashi. BET surface areas of crystals were measured by nitrogen gas adsorption with continuous flow method using a gas chromatograph equipped with a TCD detector at the liquid nitrogen temperature in mixing gas of nitrogen and helium flow as the carrier gas with Shimadzu Flow sorbs 2-2300. Particle size distribution of samples was obtained after ultrasonic wave treatment with 120 W in water for 10 min. Dynamic light scattering (DLS) spectrophotometer of Photal Otsuka Electronics, ELS-8000SA was used at a 90° angle. The analysis was determined by weight-based distribution.

Acidity was estimated by TPD (temperature-programmed desorption) profiles of pre-adsorbed NH_3 using with a Quadruple Mass Spectrometer (M-QA100F) of BEL Japan Adsorption of ammonia was done at above 100°C to restrain influence of water. The desorption of NH_3 was measured on mass number 16 by Q-Mass detector with a constant heating rate of 10°C/min at the temperature range from 100°C to 600°C.

3. Results and discussion

3.1. Influence of the various factors involved in gel mixture preparation

3.1.1. Influence of the mixing order (for group 1 samples)

The crystallinity of samples synthesized by various mixing methods are shown in Fig. 3. This result shows that predominantly the method (b) (SPDM) exhibits the faster and higher crystallinity, which means that the very homogeneous gel can be obtained with transparent sol type in the method (b). However, some gel mixtures by the methods (a) and (c) were semi-transparent and cloudy in mixing steps. This is ascribed to pH change in gel mixture such that the pH of gel mixture during mixing steps was very stable in gel mixture of (b) kept to pH 7, via spontaneous addition of phosphoric acid to other reagents, while the pHs in gel mixtures of (a) and (c) were abruptly changed by addition of template in final or first steps. Abrupt change of pH at gel preparation stage could already change gel mixture to dense form before hydrothermal treatment, and this mixture could be easily changed to other phase than SAPO-34. As a result, such relationship between pH and crystallization time for three methods is incurred as shown in Fig. 3. Crystallization time varied according to the mixing method, and in particular, the (b) method had the shortest time in these cases. The crystallization time was acquired by observing the corresponding peak intensity in XRD patterns; the peak intensity increased according to increase in time of hydrothermal treatment in all samples. Especially, the crystallinity was the highest after 5 h of hydrothermal treatment, and XRD intensities did not grow up afterwards. From these results, it was concluded that the crystallization already finished during 5 h at 200°C.

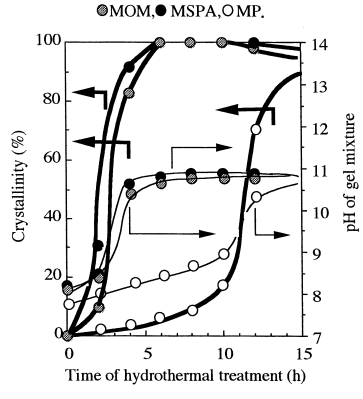

Fig. 3. Change of the crystallinity and the pH correspond to the time of hydrothermal treatment on NiAPSO-34 crystals synthesized by various mixing orders (hydrothermal treatment: 200°C). Shaded circles: OMM, full circles: SPDM, open circles: PM.

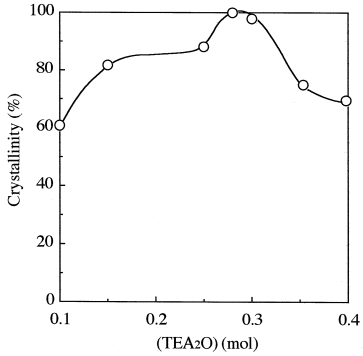

Fig. 4. Effect of template concentration on crystallinity for the NiAPSO-34 crystals synthesized by OMM (for 0.2 mol Al_2O_3).

3.1.2. Influence of the template concentration (for group 2 samples)

In synthesis by patent method, the concentration of template was just 0.2 M at 0.2 M of aluminum. The concentration of template is very important for controlling pH of gel mixture. In general, pure SAPO-34 crystal is acquired when the pH at gel preparation stage is neutral. These concentrations were ranging from 0.1 to 0.3 M at constant of aluminum concentration of 0.2 M. These results are shown in Fig. 4. When the concentration was below 0.5 M, the crystal easily changed from CHA to AFI type. On the other hand, crystals with low crystallinity and low yield were obtained over 0.35 M template concentration. The best template concentrate was 0.25 M based on 0.2 M Al_2O_3. At this point, the pH was 7.49.

3.1.3. Influence of the nickel amounts (for group 3 samples)

As depicted in Table 1, the particle size was controlled by Ni amount added. The peak intensity observed from XRD pattern explains that the crystallinity decreased with increasing Ni amount, and the increase in Ni amounts led to the small particles as shown in the SEM picture. From this result, it could be supposed that the number of nucleus was increased by addition of nickel source at gel formation stage, while the rate of crystal growth was not decreased. Therefore, addition of nickel source resulted in smaller particles. Furthermore, it can also control the acid density of the crystal. Apparently, silicon displaying acidity in crystal was replaced by nickel, and resulted in a decrease of acid sites.

3.1.4. Influence of the silica source and amount (for group 4 samples)

Fig. 5 shows particle size distribution obtained by DLS test. The particle size of sample prepared from tetraethyl orthosilicate was uniform and smaller than that from other silica sources. However, the yield was less those that with other silica sources. On the other hand, particle size distribution of the sample prepared from silica sol was wider than that from tetraethyl orthosilicate. According to Demuth et al. [14], the alumina and silica source had influence on crystal size being ascribed to differences in diffusion rates of these metal solved in water.

In Fig. 6, correlation between crystallinity and Al:Si ratio is shown. At Al:Si of 5, the crystallinity was the highest. However, for ratios above 5, the crystallinity was down again, and crystals were mixed with impurity assigned to SAPO-5. From this result, it is suggested that the Al:Si ratio control is necessary for synthesis of crystal with pure type.

Table 1
Effect of Si:Ni molar ratio on properties of NiAPSO-34 crystals

Amount of Ni (Si:Ni)	Crystallinity (for SAPO-34 100%)	Surface area (m^2/g)	Crystal size (μm)	Acid density in crystal ($\mu mol/m^2$)
100	100	585	1–1.5	4.55
40	98	565	0.7–1.0	4.05
20	73	504	0.3–0.8	2.02
Experimental methods	XRD	BET	SEM	NH_3-TPD/BET

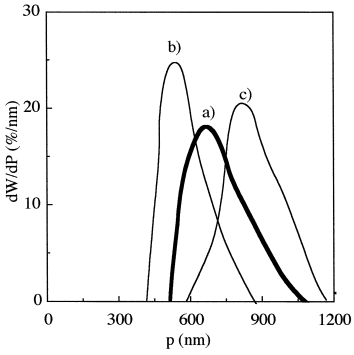

Fig. 5. Effect of silicon source on distribution of particle size for the NiAPSO-34 crystals synthesized by OMM. Used silicon source: (a) Silica sol [*a.d.:874 nm (**545)], (b) $Si(OC_2H_5)_4$ [*a.d.:622 nm (**561)], and (c) Fumed silica [*a.d.:916 nm (**547)]. *a.d.:average diameter, ** BET surface area (m^2/g).

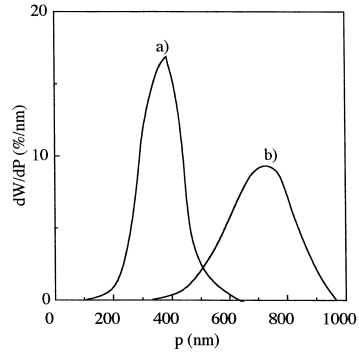

Fig. 7. Effect of seed crystal addition on the distribution of particle size. (a) With addition of seed crystal, (b) without addition of seed crystal.

3.2. Influence of factors after gel mixture preparation

3.2.1. Influence of the seed crystal addition (for group 5 samples)

Seed crystals of desired molecular sieve zeolites is commonly added to a synthesis mixture to promote crystallization of certain zeolites phases and to increase the rate of crystallization. However, the effect of seed crystal addition and the relevant crystallization mechanism have not been thoroughly assessed or understood. Fig. 7 shows that addition of seed crystal has influence on distribution of particle size. The particle size of samples with seed crystal was smaller with a sharper distribution, compared with that without seed crystal. The particle size depended on the size of seed crystal added. When the seed crystal with smaller size was used, obtained particle size decreased as well. On the other hand, the crystallinity was much higher and the crystallization rate was faster in the crystal with addition of seed crystal than that without seed crystal, as shown in Fig. 8. The measured crystallization time was similar in both samples with or without seed crystal; however, the crystallinity was higher in the sample with seed crystal. In addition, the crystallization rate was frequently enhanced by seed crystal addition to a synthesis mixture.

3.2.2. Influence of the ultrasonic wave treatment (for group 6 samples)

Although studies of ultrasonic wave treatment for precipitation product have been re-

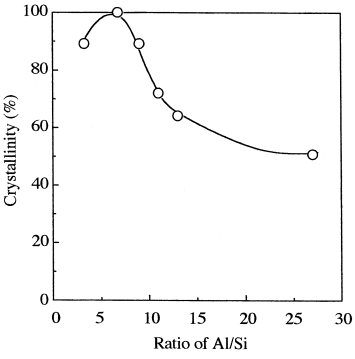

Fig. 6. Effect of Al:Si molar ratio on crystallinity for the NiAPSO-34 crystals synthesized by MOM.

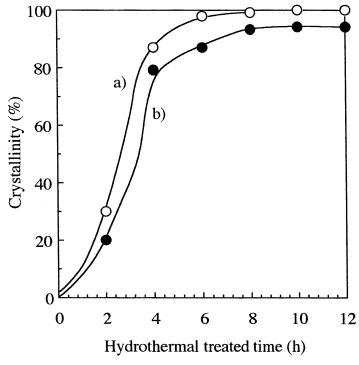

Fig. 8. Effect of seed crystal addition on crystallinity. (a) Without addition of seed crystal, (b) with addition of seed crystal.

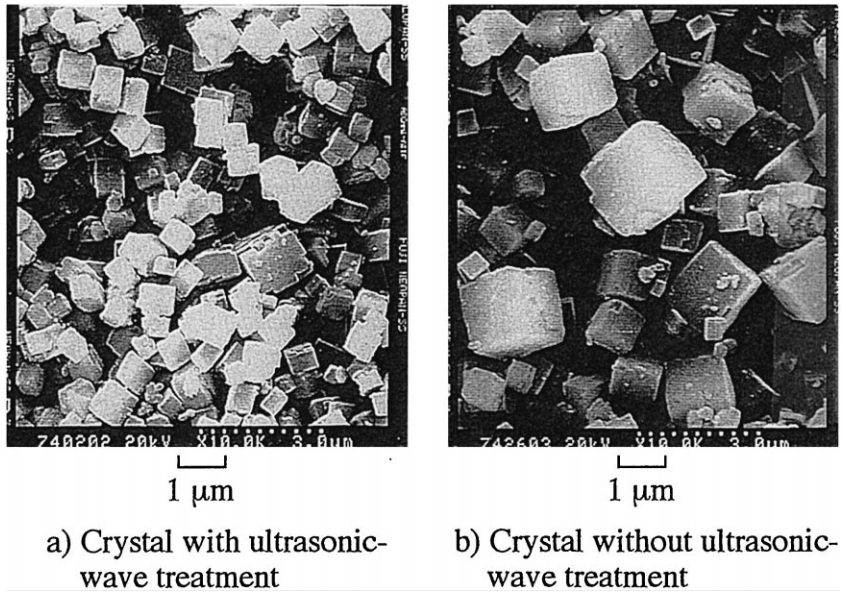

Fig. 9. Effect of ultrasonic-wave treatment on particle size.

ported, their influences were not certified. From the SEM picture in Fig. 9, the particle size of sample with ultrasonic wave treatment is 1/5 to as that without ultrasonic wave treatment. It was suggested that the number of nucleus increased, while the rate of crystal growth decreased by ultrasonic-wave treatment at gel formation stage.

The corresponding of particle size distribution are shown in Fig. 10. The particle distribution broadly dispersed around 400 nm to over 900 nm for the sample without ultrasonic wave treatment, while dispersed between 250 nm and 530 nm for that with ultrasonic wave treatment. Apparently, the gel mixture becomes of per-

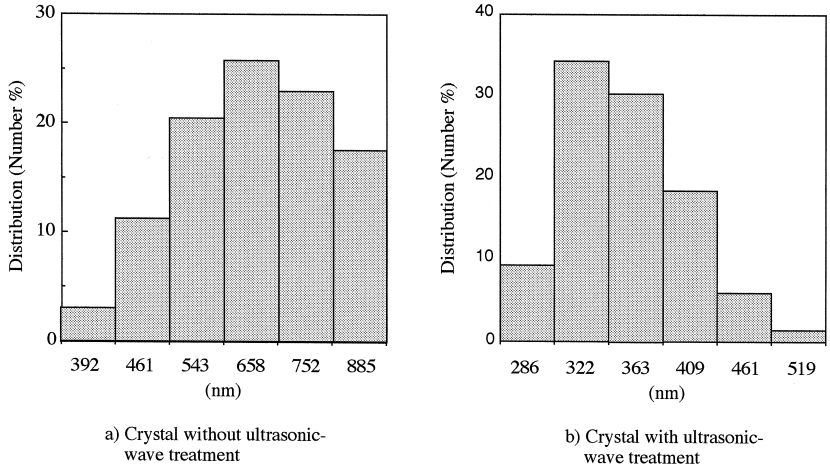

Fig. 10. Effect of ultrasonic-wave treatment on the distribution of particle size.

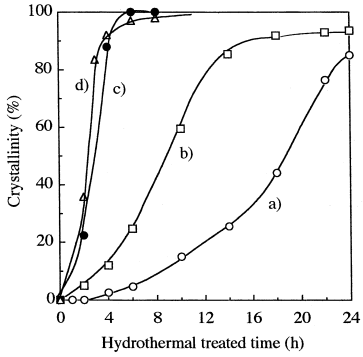

Fig. 11. Effect of various temperature on hydrothermal treatment time. (a) 150°C, (b) 170°C, (c) 200°C, and (d) 220°C.

fectly homogeneous phase by ultrasonic wave treatment before hydrothermal treatment.

3.2.3. Influence of the crystallization time (for group 7 samples)

In this work, the synthesis temperature was varied from 150°C to 220°C. It is known that the crystallization of SAPO-34 begins at 150°C, and the preferred temperature to obtain a pure phase of clear SAPO-34 crystals is around 200°C; as the higher and lower reaction temperatures lead to a dense aluminophosphate phase, similar to tridymite, a few SAPO-5 types were formed. In the report of Grebner et al. [15], the growth process of DOH crystals is discussed, and it was emphasized that most of the nucleation takes place during heating to the final reaction temperature. Furthermore, the final temperature had effects on the amount of nucleation and morphology. However, the heating rate was not considered with respect to particle size distribution. Fast heating rates cause smaller number of nuclei due to the fact that the nuclei formed grow faster and consumption of precursors from the reaction gel is accelerated. This reduces the supersaturation below the nucleation threshold, and thus, no more nuclei can be formed. However, not only particle size but also degree of purity was important. In Fig. 11, the relation between temperature of hydrothermal treatment and crystallinity are shown. The higher the hydrothermal temperature, the faster the crystallization was. However, at 220°C, the crystallization time was the shortest of 2 h, but the crystal was mixed with impurity. Obviously, proper temperature is necessary for crystallization of gel mixture. In particular, at 200°C, the pure crystal was acquired successfully in a short time.

4. Conclusion

The morphology of SAPO-type molecular sieves was influenced by many factors at the gel preparation. The mixing order was very important to control hydrothermal time and morphology. When the SAPO was synthesized by simultaneous phosphate dropping method, the crystals with CHA type were acquired with perfect cubic type, although the yield decreased. The pH was affected by template concentration, the silica source, and its amount, which controlled the rate of crystal growth and morphology. The nickel amount incorporated into the framework affected the crystal size. Excellent crystallinity was achieved by hydrothermal synthesis at 200°C. In addition, seed crystal addition (SAPO-34; 0.8 μm) and ultrasonic-wave treatment after the gel formation were effective means to generate smaller particle size with narrow size distribution.

References

[1] T.K. Das, A.J. Chandwadkar, A.P. Budhkar, A.A. Belhekar, S. Sivasankar, Micro. Mater. 4 (1995) 195.
[2] T.K. Das, A.J. Chandwadkar, A.P. Budhkar, S. Sivasankar, Micro. Mater. 5 (1996) 401.
[3] A.F. Ojo, L.B. McCusker, Zeolites 11 (1991) 410.
[4] S.T. Wilson, Surf. Sci. Catal. 58 (1991) 137.
[5] G. Finger, J.R. Mendau, M. Bulow, Zeolites 11 (1991) 443.
[6] H.-S. Han, H. Chon, Micro. Mater. 3 (1994) 331.
[7] M.G. Uytterhoeven, R.A. Schoonheydt, Micro. Mater. 3 (1994) 265.
[8] X. Ren, S. Komarneni, D.M. Roy, Zeolites 11 (1991) 142.
[9] H. Weyda, H. Lechert, Zeolites 10 (1990) 251.

[10] J.A. Martens, P.J. Grobet, P.A. Jacobs, Stud. Surf. Sci. Catal. 37 (1988) 97.
[11] W.M. Meier, D.H. Olson, Atlas of Zeolites Structure Types, 3rd edn., Butterworty-Heinemann, 1992.
[12] T. Inui, S. Phatanasri, H. Matsuda, J. Chem. Soc., Chem. Commun. (1990) 205.
[13] B.M. Lok, C.A. Messina, R.L. Patton, R.T. Gajek, T.R. Cannon, E.M. Flanigen, US Pat., 4 440 871, 1984.
[14] D. Demuth, G.D. Stucky, K. Kunger, F. Schuth, Micro. Mater. 3 (1995) 473.
[15] M.D. Grebner, A. Reich, F. Schuth, K.K. Unger, K.D. Franz, Zeolites 13 (1993) 139.